GEOLOGY | THE GEOLOGICAL SOCIETY OF AMERICA®

https://doi.org/10.1130/G46042.1

Manuscript received 25 January 2019
Revised manuscript received 14 May 2019
Manuscript accepted 15 May 2019

Effects of size-dependent sediment mixing on deep-sea records of the Paleocene-Eocene Thermal Maximum

Brittany N. Hupp[1], D. Clay Kelly[1], James C. Zachos[2], Timothy J. Bralower[3]
[1]Department of Geoscience, University of Wisconsin–Madison, 1215 West Dayton Street Madison, Wisconsin 53706, USA
[2]Earth and Planetary Sciences Department, Institute of Marine Sciences, University of California, Santa Cruz, 1156 High Street, Santa Cruz, California 95064, USA
[3]Department of Geosciences, Pennsylvania State University, 201 Old Main, University Park, Pennsylvania 16802, USA

ABSTRACT

Stratigraphic features of the carbon isotope excursion (CIE) marking the Paleocene-Eocene Thermal Maximum (PETM; ca. 55.8 Ma) are used to study ocean-climate change and carbon cycling during this ancient global warming event. Yet discrepancies in its timing and amplitude exist between bulk-carbonate and planktic-foraminifera $\delta^{13}C$ records. Here we examine these disparities through the lens of $\delta^{13}C$ compositions of size-segregated planktic shells across the pre-CIE to CIE transition in the iconic PETM section of Ocean Drilling Program Site 690 in the Weddell Sea. Our results show that the stratigraphic position of the CIE onset is dependent upon shell size, which we attribute to preferential mixing of smaller shells with pre-CIE $\delta^{13}C$ values up into the overlying CIE interval. Hence, the transitory loss of size-dependent $\delta^{13}C$ signatures in photosymbiotic planktic foraminifera is a taphonomic artifact, not a geochemical signal of symbiont "bleaching" during the PETM. Our results also indicate that many salient features of the Site 690 bulk-carbonate $\delta^{13}C$ record are aberrations caused by size-dependent sediment mixing, and as such, should not be viewed as primary signals of ocean-climate change during what is arguably one of the best ancient analogs for future ocean-climate change.

INTRODUCTION

Geologic records of past global warming events are archives that inform us about future outcomes of ongoing ocean-climate change driven by fossil-fuel emissions (e.g., Zeebe and Zachos, 2013). One such event is the Paleocene-Eocene Thermal Maximum (PETM; ca. 55.8 Ma) during which Earth surface temperatures rose by ~5 °C and global biogeochemical cycles were perturbed (e.g., Kennett and Stott, 1991; Zachos et al., 2003; Bowen et al., 2004). A hallmark of the PETM is a negative carbon isotope excursion (CIE) in terrestrial and marine materials (McInerney and Wing, 2011). The cause(s) of the PETM remains controversial, but it is generally agreed that the CIE signals the rapid input of massive quantities of $\delta^{13}C$-depleted carbon into the ocean-atmosphere system (Dickens et al., 1995; Gutjahr et al., 2017).

Study of deep-sea sedimentary records yields insight into how the ocean-climate system and marine biota responded to PETM conditions, yet the fine-scale structure of these records is commonly distorted by sediment mixing and/or carbonate dissolution (e.g., Kelly et al., 1996; Ridgwell, 2007; Bralower et al., 2014). For instance, a data-model comparison recently showed that sediment mixing can account for several salient trends expressed in foraminifera stable-isotope records constructed for the archetypal PETM section of Ocean Drilling Program (ODP) Site 690, Weddell Sea (Kirtland Turner et al., 2017). Results of such sediment-mixing models heighten awareness of taphonomic biases in pelagic records of the PETM, but a key element of sediment mixing hitherto overlooked is its particle size–dependent nature. Addressing this shortcoming is important because microfossils used to construct CIE records show an order-of-magnitude size range, from 3–10 µm nannofossils to 300–355 µm foraminifera; hence, differences in the hydrodynamic and sedimentary properties of these diverse particles influence their residence times in the surficial mixing layer prior to being incorporated in the stratigraphic record (e.g., Wheatcroft and Jumars, 1987). Here we report parallel $\delta^{13}C$ records constructed with graduated series of size-segregated planktic foraminifera, affording the rare opportunity to examine how size-dependent sediment mixing manifests in the Site 690 PETM record. Our size-segregated $\delta^{13}C$ data also suggest that loss of the $\delta^{13}C$ signature of photosymbiosis in planktic foraminifera is likely an artifact of sediment mixing. Thus, failure to consider the effects of size-dependent sediment mixing can lead to erroneous paleoecological inferences pertaining to the PETM.

MATERIALS AND METHODS

Ocean Drilling Program Site 690 is located atop Maud Rise (65°9.63′S, 1°12.27′E) in the Weddell Sea and was at upper-abyssal water depths (~2000 m) during the late Paleocene (Thomas, 1990; Fig. 1). Twelve core samples

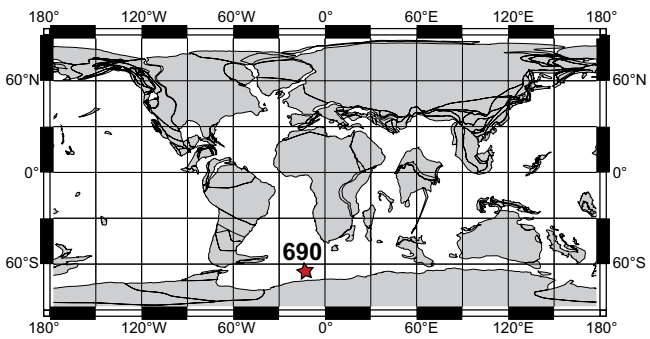

Figure 1. Location of Ocean Drilling Program Site 690 (Weddell Sea) in reference to late Paleocene paleogeography. Base map acquired from Ocean Drilling Stratigraphic Network (http://www.odsn.de).

CITATION: Hupp, B.N., Kelly, D.C., Zachos, J.C., and Bralower, T.J., 2019, Effects of size-dependent sediment mixing on deep-sea records of the Paleocene-Eocene Thermal Maximum: Geology, https://doi.org/10.1130/G46042.1

straddling the CIE onset (Fig. 2) were disaggregated using a pH-buffered sodium hexametaphosphate hydrogen peroxide (30 vol%) solution, wet sieved (>63 µm), rinsed with distilled water, and oven dried (30 °C) overnight. Shells of the planktic foraminifera species *Acarinina subsphaerica* and *A. soldadoensis* were handpicked from the following sieve-size fractions of each sample: 150–180 µm (n = 16–22 per sample), 180–212 µm (n = 12–16), 212–250 µm (n = 5–10), 250–300 µm (n = 2–4), and, whenever present, 300–355 µm (n = 1–6) and >355 µm (n = 1–4). Stable isotope analyses were performed on individual shells from the two largest size fractions and averaged for a given sample, whereas multiple shells were pooled to analyze each of the smaller size classes in a given sample. Stable isotope measurements were carried out at the University of California, Santa Cruz Stable Isotope Laboratory using a ThermoScientific Kiel IV carbonate device interfaced to a ThermoScientific MAT 253 dual-inlet gas-source isotope ratio mass spectrometer. External analytical precision for $\delta^{13}C$ measurements on this instrument was ≤0.1‰ (±2 standard deviations). All $\delta^{13}C$ data are reported in Table DR1 of the GSA Data Repository[1].

RESULTS AND DISCUSSION

The CIE has proven invaluable for correlating PETM records, yet CIE records generated with bulk-carbonate ($\delta^{13}C_{bulk}$) samples typically differ from those constructed with planktic foraminifera ($\delta^{13}C_{pf}$) in a number of ways. The amplitude of the CIE in $\delta^{13}C_{bulk}$ records is generally smaller than in $\delta^{13}C_{pf}$ records, and its onset in $\delta^{13}C_{bulk}$ records commonly occurs higher in the stratigraphy than in complementary $\delta^{13}C_{pf}$ records (Bralower, 2002; Stoll, 2005). These disparities are evident in $\delta^{13}C$ records of the Site 690 PETM section (Fig. 2), which is regarded as being the most complete deep-sea record to which other PETM records are compared (e.g., Bains et al., 1999; Röhl et al., 2007). Assigning significance to such stratigraphic vagaries is a tenuous proposition, as examination of core photographs reveals that the burrowing activity of benthic organisms (bioturbation) has disturbed the Site 690 PETM stratigraphy (Bralower et al., 2014). If the Site 690 stratigraphy has been distorted by sediment mixing, as models suggest (Kirtland Turner et al., 2017), then there should be clear evidence of it in the size-segregated $\delta^{13}C$ records herein presented.

To this end, we plotted the core depth where each size class first registers CIE values relative to the core depth of the CIE onset in the $\delta^{13}C_{bulk}$ record (Fig. 3). Plotting the $\delta^{13}C_{pf}$ data within this "relative-depth domain" shows that successively smaller shells sequentially record CIE values (~0‰) farther up through the Site 690 PETM stratigraphy. In the *A. subsphaerica* $\delta^{13}C$ records, larger shells (>300 µm) first register CIE values at –6 cm, whereas shells of the smallest size fraction (150–180 µm) first return comparable CIE values 53 cm above, at +47 cm. We attribute this "phase lag" between differing size classes to size-dependent sediment mixing, where smaller shells are preferentially displaced upsection relative to larger shells. And while the published $\delta^{13}C$ data (Thomas et al., 2002) suggest some degree of downward displacement of larger (>250 µm) shells (Fig. 2), the prevailing size-dependent pattern primarily reflects the upward mixing of smaller pre-CIE shells into the overlying CIE interval (Fig. 3).

A similar size-dependent pattern emerges from the *A. soldadoensis* $\delta^{13}C$ records, but the degree of stratigraphic separation between the different size classes is not as striking (Fig. 3). Such inter-species differences in the stratigraphic extent of this taphonomic signal likely stem from differences in the relative abundances of the two *Acarinina* taxa as indicated by mixing models (Kirtland Turner et al., 2017). For example, *A. subsphaerica* is more abundant than *A. soldadoensis* within the pre-CIE interval, whereas the opposite is true for the overlying CIE interval at Site 690 (Kelly, 2002). Hence, the probability of encountering a reworked pre-CIE shell within the CIE interval is higher for *A. subsphaerica* than *A. soldadoensis*, and the greater proportion of pre-CIE *A. subsphaerica* shells would have the net effect of displacing the CIE onset further upsection among the smaller shells of this species.

The stratigraphic offsets in the acarininid (planktonic foraminifera) $\delta^{13}C$ records (Fig. 3) suggest that finer-sized particles are more intensely mixed and preferentially displaced upward in the Site 690 stratigraphy. This finding has implications for the $\delta^{13}C_{bulk}$ record because grain-size analysis has shown that nannofossils (<10 µm) are the chief constituent of bulk carbonate in the Site 690 PETM section (Bralower et al., 2014), and other studies have shown that finer-sized particles (nannofossils) are prone to extensive upward mixing in pelagic sediments (Paull et al., 1991; Ohkouchi et al., 2002). We therefore posit that preferential mixing of fine-fraction carbonate attenuates the CIE amplitude in the $\delta^{13}C_{bulk}$ record (~2.5‰) and is the principal cause of the apparent phase lag between the $\delta^{13}C_{pf}$ and $\delta^{13}C_{bulk}$ records (Fig. 2). Attenuation of the CIE in the $\delta^{13}C_{bulk}$ record via upward displacement of pre-CIE fine-fraction carbonate would also explain why the $\delta^{13}C$ gradient between the $\delta^{13}C_{bulk}$ and $\delta^{13}C_{pf}$ curves becomes inverted over the lower CIE interval (Fig. 2). As-

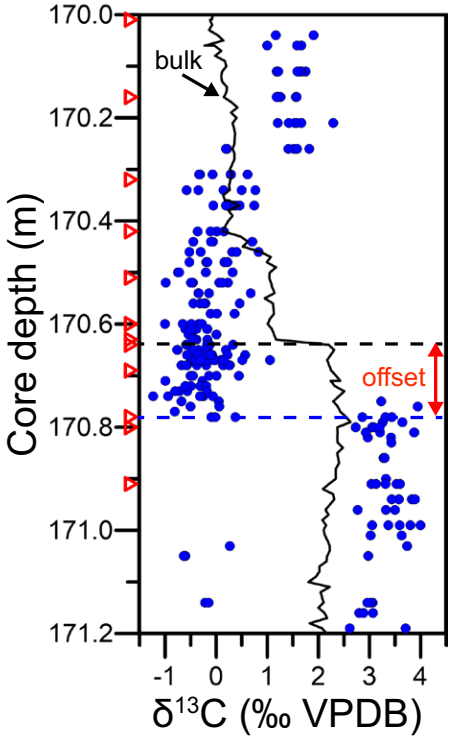

Figure 2. Chemostratigraphic records of Paleocene-Eocene Thermal Maximum carbon isotope excursion (CIE) at Ocean Drilling Program Site 690 (Weddell Sea). Planktic foraminifera $\delta^{13}C$ record is constructed with photosymbiotic acarininids (after Thomas et al., 2002) and bulk carbonate $\delta^{13}C$ record (after Bains et al., 1999). Filled circles denote values of individual shells. Open triangles mark stratigraphic positions of study samples. Horizontal dashed lines mark CIE onset in the two $\delta^{13}C$ records. VPDB—Vienna Peedee belemnite.

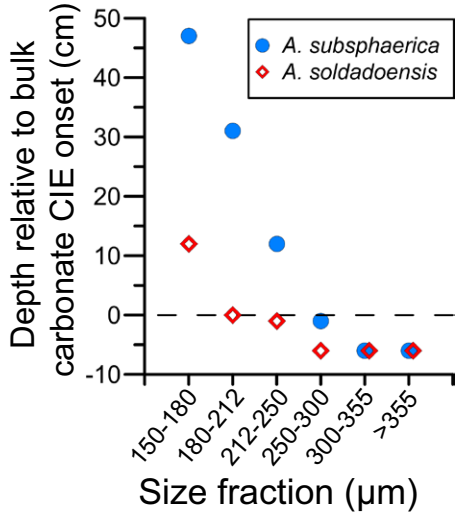

Figure 3. Stratigraphic levels of Paleocene-Eocene Thermal Maximum carbon isotope excursion (CIE) onset recorded by graduated series of shell sizes in two planktic foraminifera species at Ocean Drilling Program Site 690 (Weddell Sea). All core depths are reported relative to CIE onset in bulk-carbonate $\delta^{13}C$ record (dashed line at 0 cm). *A.*—*Acarinina*.

[1]GSA Data Repository item 2019268, geochemical data, is available online at http://www.geosociety.org/datarepository/2019/, or on request from editing@geosociety.org.

suming that differential mixing is the root cause of this transient $\delta^{13}C$ inversion, then the core depths of where the inversion initiates (i.e., CIE onset in $\delta^{13}C_{pf}$ record at 170.78 m below seafloor [mbsf]) and where "pre-CIE like" gradients are restored (~170.26 mbsf) can be used to approximate the stratigraphic reach of this taphonomic bias (~52 cm) in the Site 690 section. Clearly, size-dependent sediment mixing is not limited to the CIE onset, as pooled, multi-shell (n = 16–22) samples of small *A. subsphaerica* (150–180 µm) do not approach CIE values until +47 cm (Fig. 3).

Our size-segregated records also show that covariation between $\delta^{13}C$ values and shell size ($\delta^{13}C$-size) changes over the CIE interval (Fig. 4). Within the pre-CIE interval (Fig. 4A), all *A. subsphaerica* size classes return pre-CIE values (~3‰–4‰) and delineate a $\delta^{13}C$-size relation with a positive slope. However, $\delta^{13}C$ values of larger shells (>300 µm) abruptly decrease by ~4‰ to CIE values (~0‰) in the overlying sample (–6 cm) while shells from the four smaller size classes continue to show pre-CIE values (~3‰–3.5‰) and maintain the positive $\delta^{13}C$-size relation (Fig. 4B). The "geologically instantaneous" ~4‰ decrease registered by the larger shells (>300 µm) suggests that the base of the CIE interval may be truncated by carbonate dissolution (e.g., Dickens et al., 1997; Zachos et al., 2005), a view supported by the lack of intermediate $\delta^{13}C$ values among larger (>250 µm) acarininid shells (Thomas et al., 2002; Zachos et al., 2007). In the succeeding sample (+3 cm), shells from the three largest size fractions of *A. subsphaerica* yield CIE values, while the 212–250 µm size fraction registers a transitional value of ~2.4‰ and the two smaller size fractions (<212 µm) continue to show pre-CIE values (Fig. 4C). This sequential pattern of change, where each successive sample leads to the next smallest size fraction yielding transitional $\delta^{13}C$ values before fully transitioning to CIE values, progresses up through the CIE interval until all *A. subsphaerica* size classes converge on CIE values at +47 cm (Fig. 4E). The $\delta^{13}C$-size relation with a positive slope reappears in the uppermost sample at +62 cm (Fig. 4F).

A similar size-dependent pattern sequentially unfolds up through the CIE interval in the $\delta^{13}C$-size relation of *A. soldadoensis* (Figs. 4G–4L). Unfortunately, a paucity of *A. soldadoensis* shells—especially in the larger (>250 µm) size classes—precluded construction of the $\delta^{13}C$-size relation for this species within the pre-CIE interval. As a result, $\delta^{13}C$ data compiled for size-segregated shells of *A. soldadoensis* from a late Paleocene (pre-CIE) sample recovered at tropical ODP Site 761 (Quillévéré et al., 2001) are shown purely for illustrative purposes (Fig. 4G). This substitution is deemed appropriate because the pre-CIE values and $\delta^{13}C$-size trend delineated by these *A. soldadoensis* data are similar

Figure 4. Stratigraphic succession of size-segregated $\delta^{13}C$ records for two planktic foraminifera species, *Acarinina subsphaerica* (A–F) and *A. soldadoensis* (H–L) spanning Paleocene-Eocene Thermal Maximum carbon isotope excursion (CIE) onset at Ocean Drilling Program (ODP) Site 690 (Weddell Sea). Core depths of samples are reported relative (± cm) to CIE onset in bulk-carbonate $\delta^{13}C$ record. Horizontal dashed lines at 0‰ serve as visual aid. Dashed lines with positive slopes denote pre-CIE values and size-dependent trend for *A. subsphaerica*. Note pre-CIE values and $\delta^{13}C$-size covariation for *A. soldadoensis* shown in panel G are from Quillévéré et al. (2001) and are purely for illustrative purposes. VPDB—Vienna Peedee belemnite.

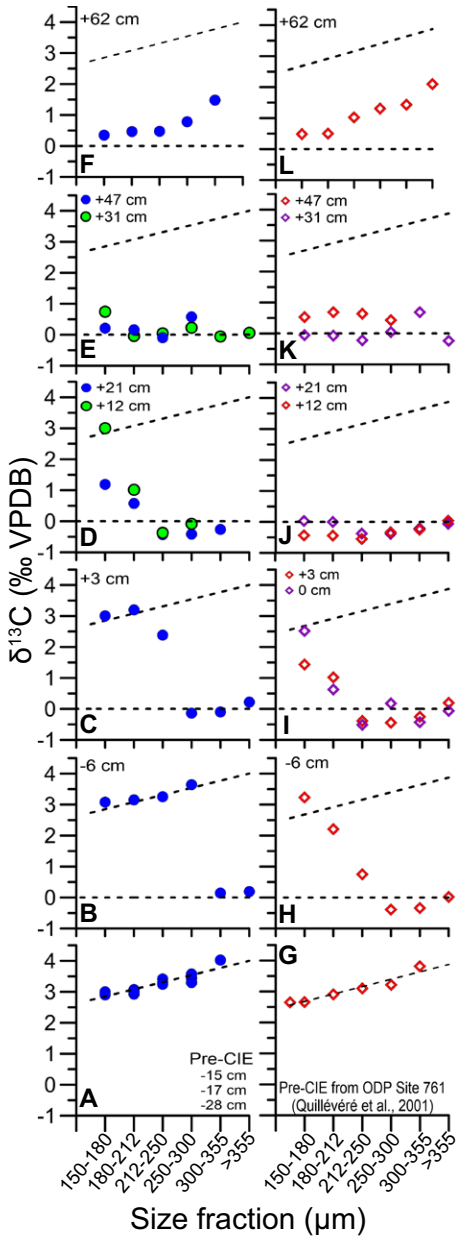

to those yielded by pre-CIE shells of *A. subsphaerica* at Site 690 (see Figs. 4A and 4G).

Comparable stratigraphic trends in $\delta^{13}C$-size covariation have been reported in the CIE interval at nearby ODP Site 689 (Maud Rise) where it was attributed to the loss of algal symbionts in response to ocean warming (Si and Aubry, 2018). This interpretation is predicated upon culturing studies of planktic foraminifera showing that the $\delta^{13}C$ signatures of extant species harboring photosymbionts exhibit a strong size dependency, with values increasing at larger shell sizes (Spero and Lea, 1993). The distinctive $\delta^{13}C$-size signature of photosymbiosis is a prevalent feature among acarininids (Quillévéré et al., 2001), so the loss of this stable-isotopic signal could be perceived as signaling a shift to paleoenvironmental conditions detrimental to marine organisms that host algal symbionts. However, sedimentological evidence indicates that the stratigraphy of the CIE interval at Site 689 has been distorted by sediment-mixing processes (Kelly et al., 2012). Further, the abrupt manner in which $\delta^{13}C$ values of larger (>250 µm) shells decrease by ~4‰, while smaller shells of *A. subsphaerica* and *A. soldadoensis* from the same samples continue to return pre-CIE values, is wholly consistent with size-dependent sediment mixing (see Figs. 4B and 4H). Even "transitional" $\delta^{13}C$ values returned by smaller size classes are readily explained by size-dependent sediment mixing as these pooled, multi-shell samples are aggregate mixtures of varying proportions of pre-CIE and CIE specimens (Figs. 4B–4E and 4H–4I).

The reappearance of positive $\delta^{13}C$-size covariation in the uppermost sample at +62 cm, which is driven by a ~1‰–2‰ increase in $\delta^{13}C$ values of larger shells, could be construed as signaling the reacquisition of photosymbionts by acarininids (Figs. 4F and 4L). Alternatively, the reestablishment of positive $\delta^{13}C$-size covariation could simply reflect the upward displacement of smaller CIE shells with low $\delta^{13}C$ values into the overlying part of the stratigraphy where $\delta^{13}C$ values of larger (>250 µm) acarininids begin to increase. We favor the latter interpretation because size-dependent sediment mixing caused the disappearance of $\delta^{13}C$-size covariation in the first place.

In summary, parallel $\delta^{13}C$ records generated with graduated series of size-segregated planktic foraminifera indicate that the upward mixing of preferentially finer-sized materials accounts for multiple discrepancies between the $\delta^{13}C_{pf}$ and $\delta^{13}C_{bulk}$ records published for the ODP Site 690 PETM section. The apparent loss of $\delta^{13}C$-size covariation signaling photosymbiosis in planktic foraminifera is a taphonomic artifact caused by differential mixing of fine- and coarse-sized materials across the CIE onset and throughout the overlying CIE interval. The results of this study also show how the combined effects of size-dependent sediment mixing and abrupt changes in the relative abundances of foraminifera taxa

affect isotopic records generated for the archetypal Site 690 PETM section, consistent with data-model comparisons. The oft-cited similarities in fine-scale structure between $\delta^{13}C_{bulk}$ records of the CIE from various sites throughout the Atlantic Ocean basin (e.g., Bains et al., 1999; Zachos et al., 2005; Röhl et al., 2007) suggest that size-dependent sediment mixing pervades the pelagic sedimentary record; hence, this taphonomic bias may not be unique to the Site 690 PETM section.

ACKNOWLEDGMENTS

Funding for this work was provided by student grants to Hupp from the American Association of Petroleum Geologists and the Geological Society of America. Thanks to Colin Carney and Dyke Andreason for technical support. This manuscript was improved by comments from three anonymous reviewers.

REFERENCES CITED

Bains, S., Corfield, R.M., and Norris, R.D., 1999, Mechanisms of climate warming at the end of the Paleocene: Science, v. 285, p. 724–727, https://doi.org/10.1126/science.285.5428.724.

Bowen, G.J., Beerling, D.J., Kock, P.L., Zachos, J.C., and Quattlebaum, T., 2004, A humid climate state during the Palaeocene/Eocene thermal maximum: Nature, v. 432, p. 495–499, https://doi.org/10.1038/nature03115.

Bralower, T.J., 2002, Evidence of surface water oligotrophy during the Paleocene-Eocene thermal maximum: Nannofossil assemblage data from Ocean Drilling Program Site 690, Maud Rise, Weddell Sea: Paleoceanography, v. 17, https://doi.org/10.1029/2001PA000662.

Bralower, T.J., Kelly, D.C., Gibbs, S., Farley, K., Eccles, L., Lindemann, T.L., and Smith, G.J., 2014, Impact of dissolution on the sedimentary record of the Paleocene-Eocene thermal maximum: Earth and Planetary Science Letters, v. 401, p. 70–82, https://doi.org/10.1016/j.epsl.2014.05.055.

Dickens, G.R., O'Neil, J.R., Rea, D.K., and Owen, R.M., 1995, Dissociation of oceanic methane hydrate as a cause of the carbon isotope excursion at the end of the Paleocene: Paleoceanography, v. 10, p. 965–971, https://doi.org/10.1029/95PA02087.

Dickens, G.R., Castillo, M.M., and Walker, J.C., 1997, A blast of gas in the latest Paleocene: Simulating first-order effects of massive dissociation of oceanic methane hydrate: Geology, v. 25, p. 259–262, https://doi.org/10.1130/0091-7613(1997)025<0259:ABOGIT>2.3.CO;2.

Gutjahr, M., Ridgwell, A., Sexton, P.F., Anagostou, E., Pearson, P.N., Pälike, H., Norris, R.D., Thomas, E., and Foster, G.L., 2017, Very large release of mostly volcanic carbon during the Palaeocene-Eocene Thermal Maximum: Nature, v. 548, p. 573–577, https://doi.org/10.1038/nature23646.

Kelly, D.C., 2002, Response of Antarctic (ODP Site 690) planktonic foraminifera to the Paleocene-Eocene thermal maximum: Faunal evidence for ocean/climate change: Paleoceanography, v. 17, 1071, https://doi.org/10.1029/2002PA000761.

Kelly, D.C., Bralower, T.J., Zachos, J.C., Silva, I.P., and Thomas, E., 1996, Rapid diversification of planktonic foraminifera in the tropical Pacific (ODP Site 865) during the late Paleocene thermal maximum: Geology, v. 24, p. 423–426, https://doi.org/10.1130/0091-7613(1996)024<0423:RDOPFI>2.3.CO;2.

Kelly, D.C., Nielsen, T.M.J., and Schellenberg, S.A., 2012, Carbonate saturation dynamics during the Paleocene-Eocene thermal maximum: Bathyal constraints from ODP sites 689 and 690 in the Weddell Sea (South Atlantic): Marine Geology, v. 303–306, p. 75–86, https://doi.org/10.1016/j.margeo.2012.02.003.

Kennett, J.P., and Stott, L.D., 1991, Abrupt deep-sea warming, palaeoceanographic changes and benthic extinctions at the end of the Palaeocene: Nature, v. 353, p. 225–229, https://doi.org/10.1038/353225a0.

Kirtland Turner, S., Hull, P.M., Kump, L.R., and Ridgwell, A., 2017, A probabilistic assessment of the rapidity of PETM onset: Nature Communications, v. 8, 353, https://doi.org/10.1038/s41467-017-00292-2.

McInerney, F.A., and Wing, S.L., 2011, The Paleocene-Eocene thermal maximum: A perturbation of carbon cycle, climate, and biosphere with implications for the future: Annual Review of Earth and Planetary Sciences, v. 39, p. 489–516, https://doi.org/10.1146/annurev-earth-040610-133431.

Ohkouchi, N., Eglinton, T.I., Keigwin, L.D., and Hayes, J.M., 2002, Spatial and temporal offsets between proxy records in sediment drift: Science, v. 298, p. 1224–1227, https://doi.org/10.1126/science.1075287.

Paull, C.K., Hills, S.J., Thierstein, H.R., Bonani, G., and Wölfli, W., 1991, ^{14}C offsets and apparently non-synchronous $\delta^{18}O$ stratigraphies between nannofossil and foraminiferal pelagic carbonates: Quaternary Research, v. 35, p. 274–290, https://doi.org/10.1016/0033-5894(91)90073-E.

Quillévéré, F., Norris, R.D., Moussa, I., and Berggren, W.A., 2001, Role of photosymbiosis and biogeography in the diversification of early Paleogene acarininids (planktonic foraminifera): Paleobiology, v. 27, p. 311–326, https://doi.org/10.1666/0094-8373(2001)027<0311:ROPABI>2.0.CO;2.

Ridgewell, A., 2007, Interpreting transient carbonate compensation depth changes by marine sediment core modeling: Paleoceanography, v. 22, PA4102, https://doi.org/10.1029/2006PA001372.

Röhl, U., Westerhold, T., Bralower, T.J., and Zachos, J.C., 2007, On the duration of the Paleocene-Eocene thermal maximum (PETM): Geochemistry Geophysics Geosystems, v. 8, Q12002, https://doi.org/10.1029/2007GC001784.

Si, W., and Aubry, M.P., 2018, Vital effects and ecologic adaptation of photosymbiont-bearing planktonic foraminifera during the Paleocene-Eocene Thermal Maximum, implications for paleoclimate: Paleoceanography and Paleoclimatology, v. 33, p. 112–125, https://doi.org/10.1002/2017PA003219.

Spero, H.J., and Lea, D.W., 1993, Intraspecific stable isotope variability in the planktic foraminifera *Globigerinoides sacculifer*: Results from laboratory experiments: Marine Micropaleontology, v. 22, p. 221–234, https://doi.org/10.1016/0377-8398(93)90045-Y.

Stoll, H.M., 2005, Limited range of interspecific vital effects in coccolith stable isotopic records during the Paleocene-Eocene thermal maximum: Paleoceanography, v. 20, PA1007, https://doi.org/10.1029/2004PA001046.

Thomas, D.J., Zachos, J.C., Bralower, T.J., Thomas, E., and Bohaty, S., 2002, Warming the fuel for the fire: Evidence for the thermal dissociation of methane hydrate during the Paleocene-Eocene thermal maximum: Geology, v. 30, p. 1067–1070, https://doi.org/10.1130/0091-7613(2002)030<1067:WTFFTF>2.0.CO;2.

Thomas, E., 1990. Late Cretaceous through Neogene deep-sea benthic foraminifers (Maud Rise, Weddell Sea, Antarctica), *in* Barker, P.F., et al., eds., Proceedings of the Ocean Drilling Program, Scientific Results, Volume 113: College Station, Texas, Ocean Drilling Program, p. 571–594, https://doi.org/10.2973/odp.proc.sr.113.123.1990.

Wheatcroft, R.A., and Jumars, P.A., 1987, Statistical re-analysis for size dependency in deep-sea mixing: Marine Geology, v. 77, p. 157–163, https://doi.org/10.1016/0025-3227(87)90090-9.

Zachos, J.C., Wara, M.W., Bohaty, S., Delaney, M.L., Petrizzo, M.R., Brill, A., Bralower, T.J., and Premoli-Silva, I., 2003, A transient rise in tropical sea surface temperature during the Paleocene-Eocene Thermal Maximum: Science, v. 302, p. 1551–1554, https://doi.org/10.1126/science.1090110.

Zachos, J.C., et al., 2005, Rapid acidification of the ocean during the Paleocene-Eocene Thermal Maximum: Science, v. 308, p. 1611–1615, https://doi.org/10.1126/science.1109004.

Zachos, J.C., Bohaty, S.M., John, C.M., McCarren, H., Kelly, D.C., and Nielsen, T., 2007, The Palaeocene-Eocene carbon isotope excursion: Constraints from individual shell planktonic foraminifer records: Philosophical Transactions of the Royal Society A, v. 365, p. 1829–1842, https://doi.org/10.1098/rsta.2007.2045.

Zeebe, R.E., and Zachos, J.C., 2013, Long-term legacy of massive carbon input to the Earth system: Anthropocene versus Eocene: Philosophical Transactions of the Royal Society A, v. 371, https://doi.org/10.1098/rsta.2012.0006.

Printed in USA